1990

Mismatching Noise Source Spectrum and Resonance Spectrum of Reciprocating Compressor Shells

M. B. Laursen
Danfoss-Flensburg GmbH

Mismatching Noise Source and Resonance Spectra of Reciprocating Compressor Shells

by

M. B. Laursen, Ph.D.

Danfoss–Flensburg GmbH
D–2390 Flensburg, F.R.Germany

ABSTRACT

The feasibility of spectral mismatching of noise source and shell resonance spectra of a hermetic reciprocating compressor is investigated. The concept of local reshaping is introduced as a means to protect investments in existing compressor types. The potential of this approach is illustrated through parametric surveys of resonant frequencies belonging to three types of reinforcement structures, typical of reciprocating compressor shells. The employment of Finite Element Analysis is vital to reduce prototyping and turnaround time. Finally, a case study comprising two design iterations indicates the practical value of local reshaping.

INTRODUCTION

Low noise radiation of small hermetic compressors for domestic appliances has long been a primary performance measure. From an end–customer point of view, it may not seem worthwhile to further reduce the noise level of today's compressors. From a manufacturer point of view, growing demands on energy efficiency and the current substitution of CFCs tend to raise the noise level, as most noise–reducing measures counteract energy efficiency. Therefore, noise reduction will remain a key issue in compressor design and still more advanced analysis techniques will be needed in order to meet environmental regulations without sacrificing comfort.

When planning a new compressor range the opportunity to design a completely new shell should be taken. Annual production figures are to be counted in millions implying large long term investments in customized manufacturing equipment on part of the compressor manufacturer and to some extent his customers. Not only investments but also several functional constraints are tied to the very shape of the shell. Therefore, to protect investments and to avoid redesigning an otherwise well performing compressor range, a new shell should violate as few constraints as possible.

PROBLEM DESCRIPTION

Any hermetic compressor creates acoustic noise radiated through connecting pipes to the appliance and through the shell to the surrounding air. Airborne noise may even today prove annoying to humans although the overall level lies below agreed limits. The annoyance is attributed to distinct frequency bands of comparatively large amplitude which in some cases due to small bandwidth contribute only slightly to the overall level. The sound power level spectrum of a reciprocating compressor sample shown on fig. 1 is characterized by a 500 Hz peak attributable to standing waves in the shell cavity and a band of discrete peaks ranging from 2 to 6 kHz, having a more complex origin. The standing waves of the shell cavity induce rigid body motion of the shell structure and the comparatively large forces involved cannot be reasonably dampened once the shell is excited. Dissipative dampers applied within the cavity are precluded, as they are likely to impede the internal oil borne heat transport from the pump to the shell body. The remedies left are to reduce the sources at 500 Hz or to smear out the cavity resonance energy over a broader band by giving the shell a very irregular shape (i.e. no distinct wavelength). The latter approach may very likely violate indispensable constraints and the former lies beyond the scope of this paper.

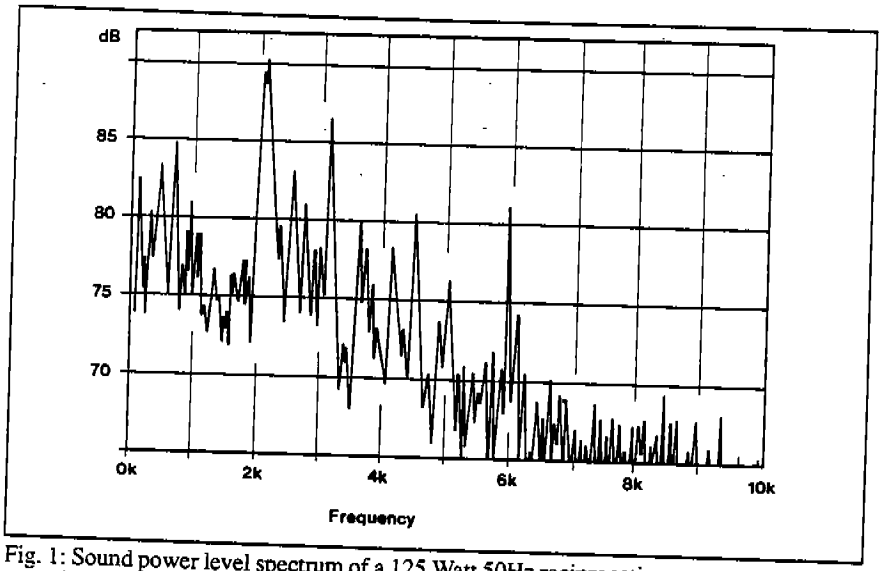

Fig. 1: Sound power level spectrum of a 125 Watt 50Hz reciprocating compressor running at performance rating conditions.

SPECTRAL MISMATCHING

Spectral mismatching is to compare noise source and shell resonance spectra, localize the dominant noise peaks and then redesign the shell so the peaks of the two spectra do not coincide. This approach will be demonstrated through a case study of the abovementioned compressor sample.

A prerequisite for spectral mismatching to work is the existence of a good correlation between noise source, shell resonance and radiated noise spectra. The sound power spectrum of an open (no shell) compressor running at normal load and one of an empty shell excited by white noise (through a loudspeaker placed in the cavity) is shown on fig. 2. The noise spectra turned out to be very sensitive to microphone location, but a pattern of dominant peaks did emerge. The noise source and radiation correlates with respect to the 2150 Hz and 3150 Hz peaks whereas the peaks at 1500 Hz and 5500 Hz did not come through. The trough between 3150 Hz and 5500 Hz on the source spectrum (fig. 2:left) emerges as several intermediate peaks on the radiation spectrum (fig. 1). These peaks were present on other open compressor spectra, were however omitted due to space limitations.

The white noise excitation of the empty shell charts the resonances (fig. 2:right). Holographic interferometry reveals the peaks at 1.8–1.9 kHz to be caused by the free–end connecting pipes and may thus be neglected. The next twelve peaks occur at {2690, 2820, 3070, 3230, 3560, 3650, 3810, 4020, 4230, 4290, 4480, 4590} Hz and are identified as shell resonances.

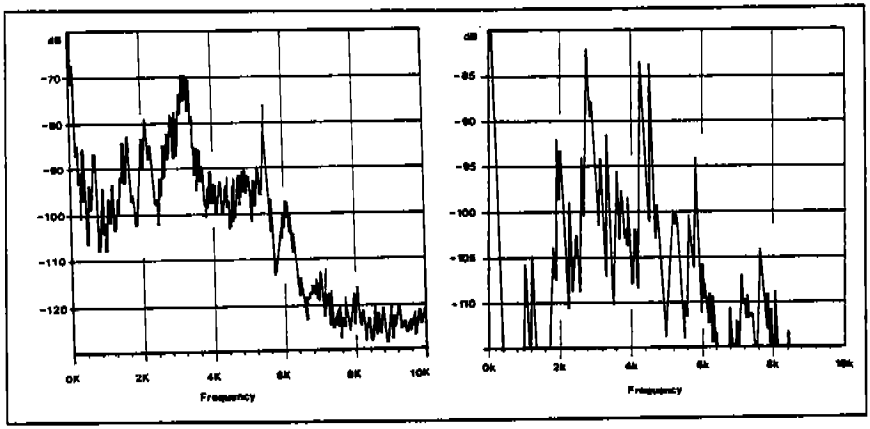

Fig. 2: Left: Noise spectrum of the open sample compressor. Right: the radiated noise spectrum of an empty shell excited by white noise within the cavity.

At first, there seems to be a poor correlation as the first major peak of the noise spectra occurs at 2150 Hz but the lowest resonance of the empty shell occurs at 2690 Hz. The missing link is the oil reservoir situated on the shell bottom where also the lowest mode happens to be found. The influence of oil charge amount on the lowest resonance frequency has been measured (fig. 3) on a particular shell and a significant decrease is observed. The decrease is due to the zero–stiffness mass contribution of the oil, and will only be present at modes belonging to the shell bottom. The oil charging at delivery decreaese the first mode from 2600 Hz to 2130 Hz making the abovementioned discrepancy vanish.

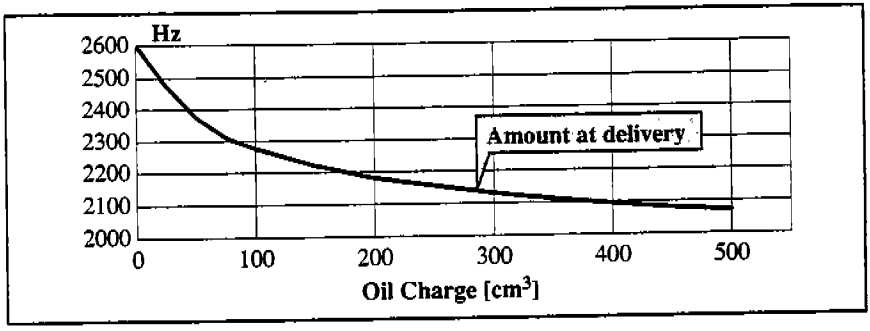

Fig. 3: Change in lowest shell resonance frequency vs. oil charge amount.

Although tempting, spectral mismatching may turn out to be infeasible as it presupposes 1) spectral stability of noise and shell resonance against manufacturing variations and 2) ability to control the resonance spectral distribution. Ad 1: Measurements of shells from different suppliers have shown deviations of about 100 Hz on the lowest mode, i.e. of the same order as the resonance separation listed above. So unless the manufacturing process is tightly controlled, spectral mismatching may be rendered useless. Ad 2: Using Finite Element Analysis (FEA), it is fairly easy to control a few resonances one at a time, but to control say 10 closely spaced resonances concurrently is impractical. If the resonance density happens to be high it should at first be thinned by the source reduction and then spectral mismatching might be sensibly applied.

LOCAL RESHAPING

The compressor shell of today is only partly optimized as noise minimization is but one of several objectives or constraints involving the shell shape. Often the objectives in constraining one another lead to a design characterized by large shallow regions blended together by narrow regions of large curvature (see sketch below). The blending regions tend to act as dynamic "nodelines" and the flexural motion takes place almost entirely in the shallow regions. When the blending region has double curvature which is often the case, the shallow regions will have a high degree of flexural independence. Flexural interaction would imply that moments in the shell midsurface be transmitted undispersed across the blending region. The receiving blending region perceives a transmitted moment as a boundary moment and on a shell of curvature $1/R$ it will be selfequilibrating with a decay half-length normal to the boundary of the order $\sqrt{R\,t}$ (t being the shell thickness). Blending regions have curvature of the order $(10\text{ mm})^{-1}$ and thickness of 3 mm yielding a decay half-length of 5 mm. The transmitted moment will simply be absorbed in the blending region, being converted into membrane forces.

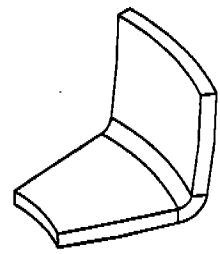

This property makes it possible to consider the shallow regions (which we term subshells) independently of one another. Determining the resonance modes of an actual shell, each mode can be referred to at least one subshell. When a particular mode appears flexurally in more subshells it is not a sign of interaction but merely of the fact that several subshells possess similar thickness, extension and curvature. The modification on subshell level is termed local reshaping.

The purpose of shell shaping is to convert vibrational bending energy into membrane energy as a shell has a much larger storage capacity of the latter. The purpose of local reshaping is to determine the modes of interest of the current shell (using either FEA, modal analysis or holographic interferometry) and to identify each mode with one or more subshells. Then the mode(s) in question may be altered by reshaping the corresponding subshell(s). To assist in selecting an appropriate local reshaping, three types of reinforcement structures will be analyzed.

First the resonances of a simply supported rectangular plate, known from elementary textbooks on thin shell theory, will be considered. The eigenfrequencies are given by

$$f_{m,n} = \frac{\pi}{2}\left(\left(\frac{m_x}{L_x}\right)^2 + \left(\frac{m_y}{L_y}\right)^2\right)\left(\frac{E\,t^2}{\rho\,12\sqrt{(1-\nu^2)}}\right)^{1/2} \qquad [1]$$

where E is modulus of elasticity, ν is Poissons ratio, ρ is mass density, t is plate thickness, L_x, L_y are plate widths and m_x, m_y are mode numbers in x– or y–direction. We rearrange eqn. 1 into the form

$$\begin{aligned} f_{m,n} &= F_0\ \Phi(m_x, m_y, \beta) \\ F_0 &= \frac{\pi}{2}\,\frac{t}{L_x^2}\left(\frac{E}{\rho\,12\sqrt{(1-\nu^2)}}\right)^{1/2} \qquad [2] \\ \Phi &= m_x^2 + \left(\frac{m_y}{\beta}\right)^2 \\ \beta &= L_y / L_x \end{aligned}$$

The spectral distribution of $f_{m,n}$ for any plate may be represented by the dimensionless frequency Φ and the dependence on the width ratio β is shown on fig 4. The density is sensitive to β and has a minimum for $\beta = 1$, ie. a square plate. The bifurcations occuring as β "leaves" 1 are due to the concurrent loss of a symmetry plane. The number of mode shapes does not change in the vicinity of $\beta = 1$, as two eigenmodes share the same eigenfrequency. In that case, high excitation is to be expected because a larger area of the plate participates effectively in the flexural motion. Therefore, a high degree of symmetry is undesirable. On the other hand, larger values of β will attract more mode shapes from regions beyond the frequency range of interest (see fig. 4). Conclusively, one has to balance the number of mode shapes against an even distribution to smear out noise peaks.

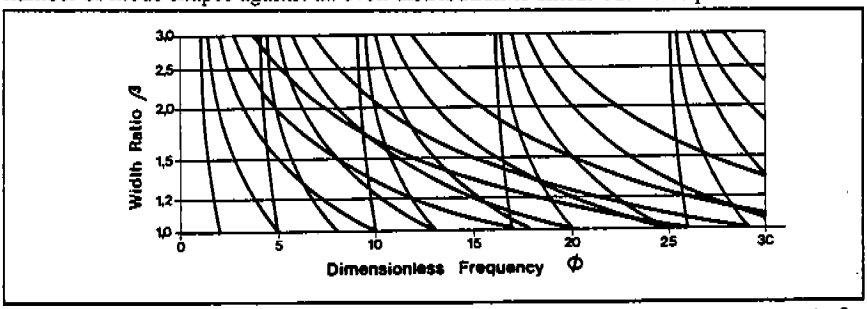

Fig. 4: Spectral distribution of dimensionless plate eigenfrequencies Φ vs. width ratio β.

The rectangular plate rarely appears as a subshell in any compressor type, but the qualitative aspects of the eigenmode behavior may be transferred to shallow subshells with irregular boundaries, as the behavior is primarily controlled by width L and thickness to width ratio t/L.

We shall now return to the abovementioned reinforcements. The three types are 1) an axisymmetric dome, 2) a triple–ribbed disc and 3) a single–ribbed square plate, each of which is defined by a few geometrical parameters. A parametric survey of the two lowest modes (#1 and #2) has been carried out using FEA, and the two eigenfrequencies f_1 and f_2 are compared to the lowest frequency f_0 of the corresponding flat configuration. Thickness variation across the structure caused by the deep–drawing process has not been taken into account leading to a slight overestimate of the frequency ratios f_1/f_0 and f_2/f_0.

The intent is to assess the potential of a given reshaping in terms of gain in mode 1 frequency and the distance to mode 2. These ratios of eigenfrequencies are presented as functions of dimensionless parameters, but have been computed using a fixed extension (radius or length) of the structure. In case of a rectangular plate, the extension parameters L_x and L_y cancel out in taking frequency ratios cf. eqn. [1]. The validity of using dimensionless parameters is assumed to hold good in the following three cases.

Dome: The height ranges from shallow dome to hemisphere and one notices that the first and second eigenfrequencies approach one another as H/R increases, to coincide for some value between 60 and 80%. This is caused by a change in mode shape from an axisymmetric to a diameter symmetric one. One may also notice the minor decrease in frequency ratio as H/R passes beyond 80%; this is due to the increasing flexural span in combination with change of mode shape.

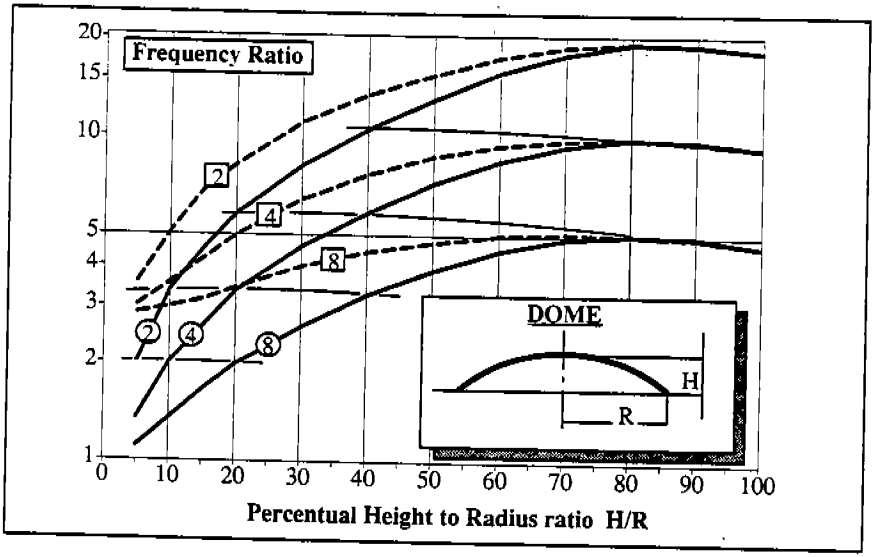

Fig. 5: Axisymmetric dome. The frequency ratios f_1/f_0 and f_2/f_0 shown in fat solid and dashed rule, respectively. Curves of constant H/t are shown for f_1/f_0 in thin rule. Percentual thickness to radius ratio t/R is shown in circles for f_1/f_0 and in squares for f_2/f_0.

Along curves of constant H/t (shown in thin rule on fig. 5) the frequency ratios are nearly independent of t/R and H/R, that is frequency gain is primarily controlled by the ratio H/t (for any fixed value of R) and the effect is most pronounced at lower values of H/R which in turn are the most relevant to local reshaping. Note, that the chart may also be used to assess the effect of modifying an existing dome.

Triple–ribbed disc: This structure (sketched on fig. 6) gives lesser gain than the dome considering equal ratios H/t as well as lesser gain in separation of the two lowest frequencies. Differences in gain diminishes as width increases, because the triple–ribbed disc becomes a dome in the limit of W. The strong dependency of H/t is also noticed for this structure.

Single–ribbed plate: This structure (sketched on fig. 7) displays a broader range of W/L ratio than the triple–ribbed disc. The width turns out to have modest influence which is advantageous from a redesign point–of–view as more ribs then may be added to a given area. The ratio f_2/f_0 is nearly independent on H/L because the 2nd mode has a nodeline along the symmetry plane perpendicular to rib width. The strong dependency of H/t is once again noticed.

Of the three structures, the dome appears to have to biggest potential in increasing the both of the two lowest resonance frequencies, whereas the 2nd mode is less affected in case of the two rib structures. This suggests domes to be applied in the first reshaping iteration and ribs to be applied if fine–tuning of the lowest mode becomes necessary.

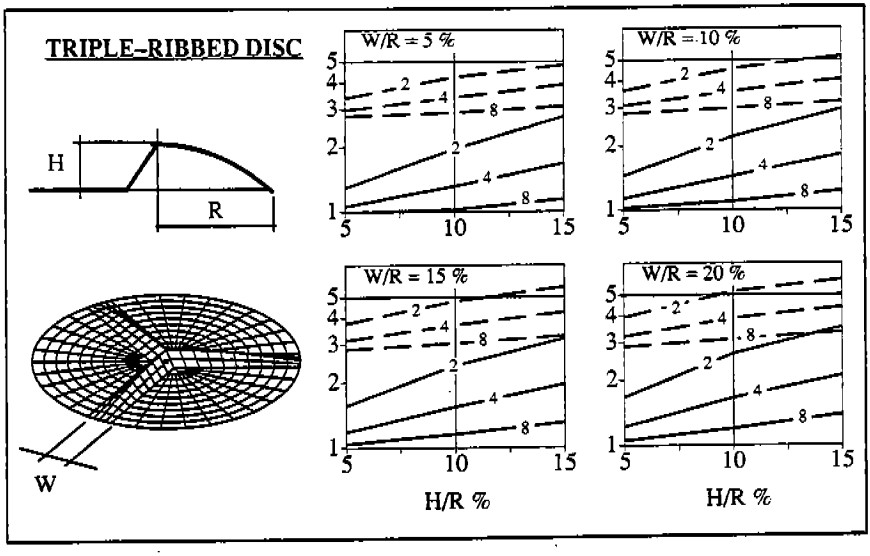

Fig. 6: Triple–ribbed disc: Parameters are rib width W, height H and plate thickness t . The frequency ratios f_1/f_0 and f_2/f_0 are shown in solid and dashed rule, respectively. Percentual values of thickness to radius ratio t/R are annotated each curve.

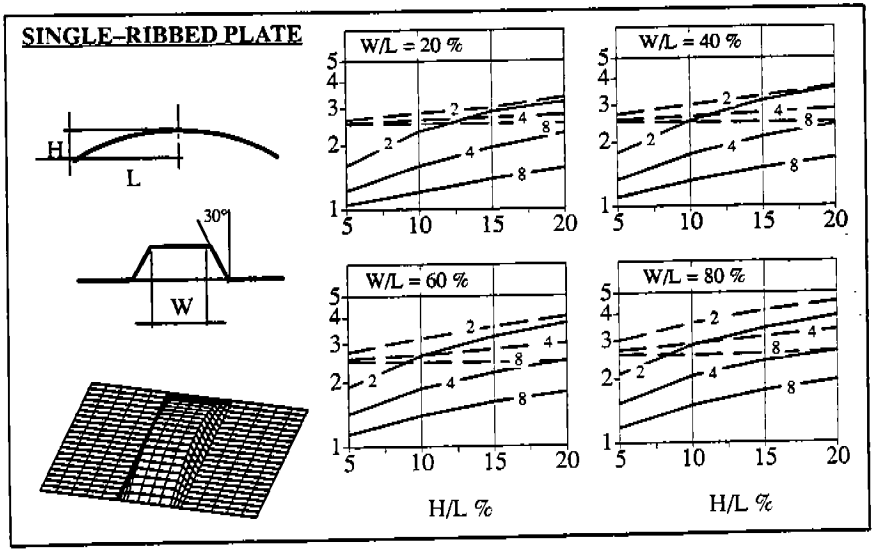

Fig. 7: Single–ribbed plate: Parameters are rib width W, height H and plate thickness t . The frequency ratios f_1/f_0 and f_2/f_0 are shown in solid and dashed rule respectively. Percentual values of thickness to radius ratio t/L are annotated each curve.

CASE: LOCAL RESHAPING OF SAMPLE SHELL

The abovementioned approach of local reshaping has been applied to the sample compressor. The lowest eigenmodes were measured through acoustic point impedance and by holographic interferometry (fig. 8) and finally computed by FEA (fig. 10). The shell FEA–model does not comprise mounting brackets as these are spotwelded onto the shell thus contributing only slightly to stiffness. Their mass contribution has been measured to be of negligible influence on the lower modes (fig. 8:left).

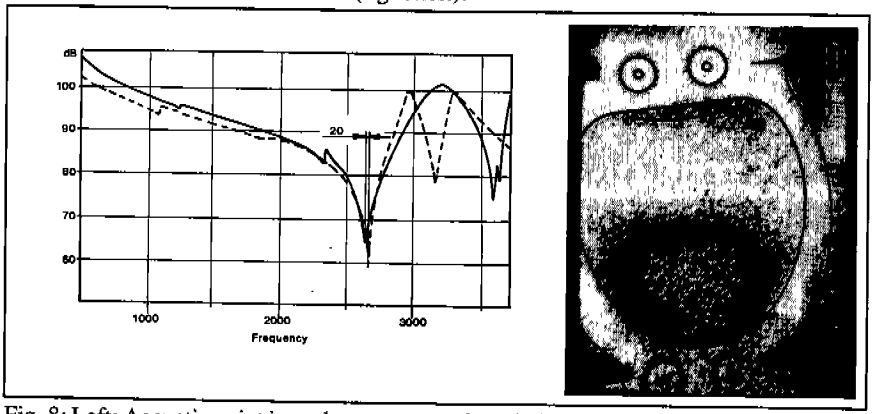

Fig. 8: Left: Acoustic point impedance measured on shell bottom without mounting brackets (solid) and with (dashed). Right: Fringe pattern on shell bottom obtained by holographic interferometry (shell contours are emphasized for clarity).

The FE–Analysis determines the undamped free vibrations of an unrestrained shell neglecting the mass of the oil charge. To save computer resources, only one–half of the symmetric shell was modeled and the terms symmetric and antimetric mode refer to mode shapes, which are symmetric and antimetric respectively across the shell symmetry plane. The symmetric half of the shell was discretized into 2500 elements comprising 9000 degrees–of–freedom, assuring that pseudo stiffness due to inadequate deformation capability of a too coarse element mesh was eliminated. The lower six eigenmodes were computed for the symmetric as well as for the antimetric deformation pattern (fig. 9).

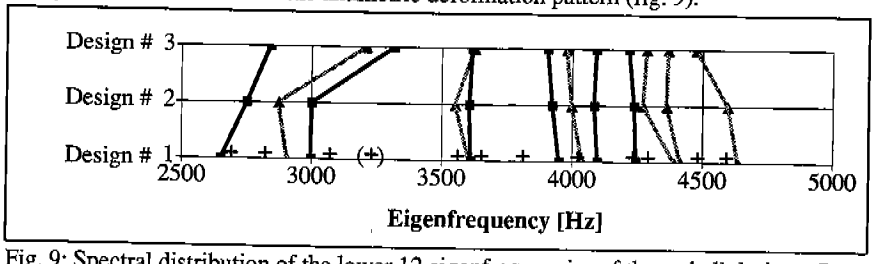

Fig. 9: Spectral distribution of the lower 12 eigenfrequencies of three shell designs. Symmetric frequencies shown in black rule and antimetric in grey rule. The resonance frequencies of the normal shell (#1) extracted from fig. 2:right are represented by '+' markers.

The correlation between measurements and FEA is illustrated on fig. 9. The computed frequencies lie within reach of the ones extracted from fig. 2:right. The deviations are attributed to manufacturing variation and coarse mapping of shell thickness variation onto the FEA–model. The measured resonance at 3230 Hz is attributed to the mounting brackets, which according to fig. 8:left cause a peak at that location. In spite of these minor deviations, we feel confident in the possibility of completing a design before actually verifying the results on physical prototypes.

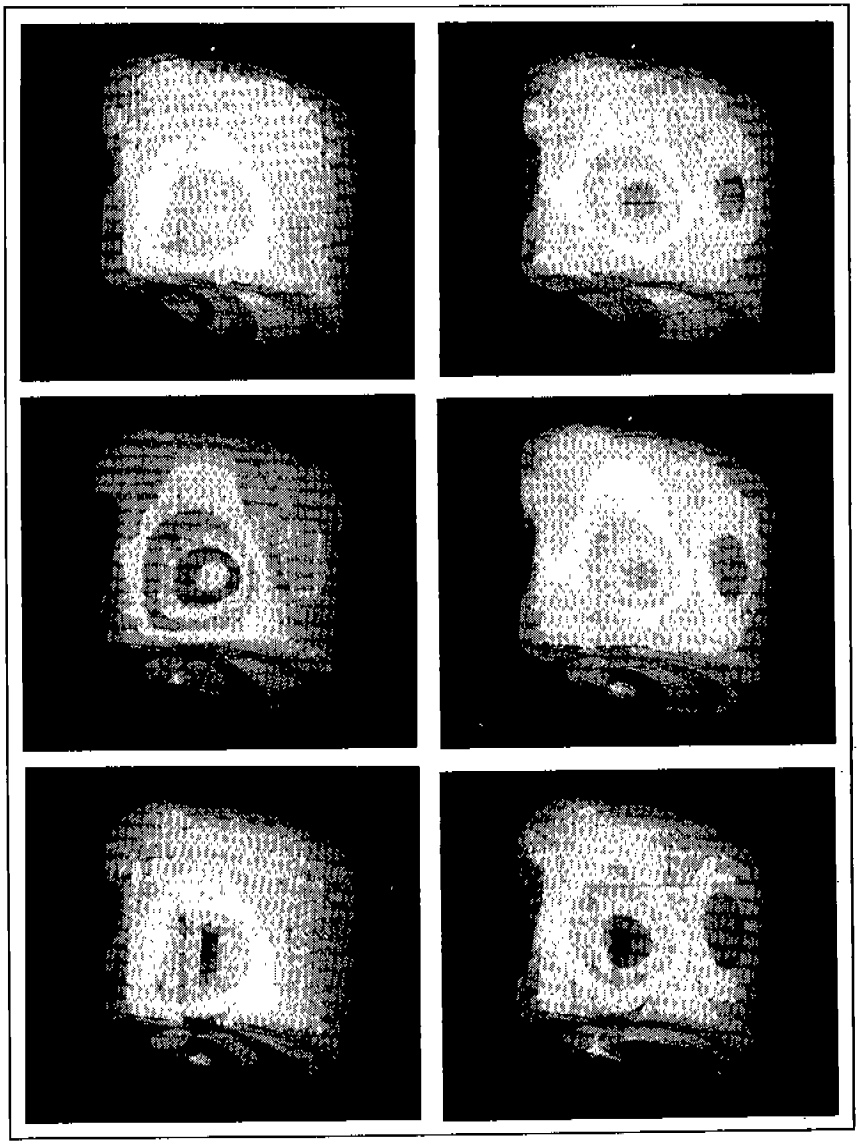

Fig. 10: From left to right: First and second symmetric eigenmode shape computed by FEA.
Upper row: Design #1 Normal shell (2651 and 2996 Hz).
Middle row: Design #2 Hammer shaped rib applied to bottom shell (2751 and 3000 Hz).
Lower row: Design #3 Additional rib applied to side region (2841 and 3300 Hz).

Three designs were analysed: #1 is the actual (normal) shell of which measurements have already been shown, #2 has had a hammer–shaped rib stamped into the bottom subshell at the locus of mode 1 of design #1 (see fig. 10), and #3 has an additional rib protruding from a side subshell at the locus of mode 1 of design #2 (see fig. 10).

In this case study, the aim was to displace resonances from the 2150 Hz and 3150 Hz peaks (see fig. 2:left) without violating any constraints. As seen on fig. 9, the lowest mode remained below 2850 Hz and we succeeded in pushing mode 2 and 3 above 3200 Hz so that all three lie on either side of the 3150 Hz peak. The other nine modes but one are practically unaltered. As mode 1 happens to prevail on the bottom subshell in design #1 and #3, it will be notable displaced by the oil charge cfr. fig. 3. Mode 2 and 3 prevails in the side subshell and are thus unaffected by the oil.

The outcome of this case study indicates the opportunities offered by local reshaping showing that success may be obtained even with modest shape modifications.

CONCLUSION

Local reshaping has shown to be feasible presuming that the noise source and shell resonance spectra are stable with respect to manufacturing variations and compressor running conditions. The entire process of analysis (noise measurement and Finite Element Analysis) also should be carried out with outmost care, if important peaks or the predictive power of FEA shall not be lost. The influence of oil charge on resonance modes appearing on the shell bottom has been shown to be significant and should be considered when judging which subshells to modify. Among local reinforcement structures, the dome possesses a large potential in increasing resonance frequencies and should be applied to the full extent. Ribs stamped into the shell body are more adequate for spectral fine–tuning purposes.